



Article

Joint Antenna Placement and Power Allocation for Target Detection in a Distributed MIMO Radar Network

Cheng Qi * , Junwei Xie and Haowei Zhang

Air and Missile Defense College, Air Force Engineering University, Xi'an 710051, China; xjw_xjw123@163.com (J.X.); zhw_xhzhf@163.com (H.Z.)

* Correspondence: qc_afeu@163.com

Abstract: Radar network configuration and power allocation are of great importance in military applications, where the entire surveillance area needs to be searched under resource budget constraints. To pursue the joint antenna placement and power allocation (JAPPA) optimization, this paper develops a JAPPA strategy to improve target detection performance in a widely distributed multiple-input and multiple-output (MIMO) radar network. First, the three variables of the problem are incorporated into the Neyman–Pearson (NP) detector by using the antenna placement optimization and the Lagrange power allocation method. Further, an improved iterative greedy dropping heuristic method based on a two-stage local search is proposed to solve the NP-hard issues of high-dimensional non-linear integer programming. Then, the sum of the weighted logarithmic likelihood ratio test (LRT) function is constructed as optimization criteria for the JAPPA approach. Numerical simulations and the theoretical analysis confirm the superiority of the proposed algorithm in terms of achieving effective overall detection performance.

Keywords: antennas placement; convex optimization; distributed MIMO radar; mixed-integer non-linear programming; power allocation; target detection



Citation: Qi, C.; Xie, J.; Zhang, H.

Joint Antenna Placement and Power Allocation for Target Detection in a Distributed MIMO Radar Network. *Remote Sens.* **2022**, *14*, 2650. <https://doi.org/10.3390/rs14112650>

Academic Editor: Okan Yurduseven

Received: 14 April 2022

Accepted: 30 May 2022

Published: 1 June 2022

Publisher's Note: MDPI stays neutral with regard to jurisdictional claims in published maps and institutional affiliations.



Copyright: © 2022 by the authors. Licensee MDPI, Basel, Switzerland. This article is an open access article distributed under the terms and conditions of the Creative Commons Attribution (CC BY) license (<https://creativecommons.org/licenses/by/4.0/>).

1. Introduction

1.1. Background and Related Studies

The detection theory development and system optimization utilization of distributed MIMO radars is one of the most important directions in metrology for radar. Multi-Input Multi-Output (MIMO) radar networks have recently received significant attention due to their superior detection and tracking performance compared to traditional monostatic radar systems [1–3]. They also possess superior anti-stealth, anti-destroy, and anti-interference performance by cooperating multiple subarrays with transmitting independent and orthogonal waveforms [4,5]. As an important category of the MIMO radar network [6], the distributed MIMO radar has enhanced detection and high localization precision because its multiple transmitters and multiple receivers are sufficiently far from each other [7–10].

Among the research topics of MIMO radars, radar resource allocation is an important pot in the military field. It plays a great promotion role in the rapid deployment of self-propelled radar equipment and air defense planning in key areas, which are critical military needs with significant applications. In particular, it is utilized in air defense operations to enhance combat efficiency within the restrictions of complex battle characteristics, such as electromagnetics, topography, and hostile situations [11,12].

Antenna position deployment and transmitting power allocation are two factors concerned by the radar resource allocation, and they determine the performance of MIMO radars. However, it is a vital challenge to maximize resource consumption efficiency and radar network performance. Various research has been devoted to them. According to the focus of the method, the related studies can be classified into three categories: the system configurations [13–15], the transmitting power allocation [16–18], and the integration of the former two [19–22].

The first category is to optimize the system configuration to enhance the performance of the radar system. Considering that the antenna placement problem is NP hard [23], traditional methods for the solution are the exhaustive search and heuristic search algorithms. However, they are either computationally intensive or only performed at a local-optimal level. As a result, the greedy algorithm [13] and intelligent algorithm [14,15] are often adopted to solve the problem. Specifically, ref. [24] proposes simulation-based discrete stochastic optimization algorithms to adaptively select a better receiving antenna subset using target tracking resolution. The effects of optimizing the remaining antennas' placement on the radar performance are studied when fixing receiving antennas and transmitting antennas separately. When optimization is extended to consider both transmitting and receiving antennas, ref. [25] investigates the target velocity estimation performance of the distributed MIMO radar using the Cramér–Rao bound and finds that increasing the number of antennas and better placement can lead to better speed estimation performance. A combinatorial optimization model for the joint placement of transmitters and receivers is established in [13], and the proposed algorithm utilizes convex relaxation to obtain the approximation of the original optimal solution. Further, [26] proposes an antenna placement scheme for compressed-sensing-based collocated MIMO radars to improve the target detection performance by minimizing the sensing matrix's coherence. An optimization algorithm is proposed for iterative placement between transmitters and receivers to obtain better detection performance. Therefore, geometry configuration is crucial to the optimization on distributed MIMO radar systems that achieves a superior performance.

The second category is to adaptively optimize the transmitting power allocation. In principle, the optimal power allocation strategy is to obtain a solution based on the convex optimization theory. For example, an alternating global search algorithm is designed in ref. [16] to minimize the non-convex Cramér–Rao low bound (CRLB) of target position estimation through power allocation, and ultimately, enhance the power utilization of the distributed radar systems. Similarly, ref. [17] presents a deterministic convex power allocation scheme and transforms it into a non-linear quality model with the Karush–Kuhn–Tucker conditions. Ref. [18] proposes a novel low probability of intercept power resource allocation (LPI-PRA) scheme that delivers superior low probability of intercept (LPI) performance in terms of minimizing the total power consumption by exploiting the semi-definite programming (SDP) and Karush–Kuhn–Tucker (KKT) conditions. Further, ref. [27] studies the robust power allocation problem for multi-target tracking in the quality of service framework and proposes an iterative parallel search algorithm to solve such a non-convex optimization problem. Hence, the flexibility and excellent performance of power allocation are shown in the superior performance of the improved radar network.

The last category is joint optimization of the former two items. The research on the joint antenna placement and power allocation in MIMO radars also yielded fruitful results. For instance, ref. [28] proposes a suboptimal, but computationally efficient, method for scheduling and power allocation based on greedy programming in multi-target tracking. It improves tracking accuracy by adopting the suitable subset of antennas to be employed in each tracking interval, as well as the power transmitted by these antennas. In addition, ref. [19] establishes the SNR criteria for the antenna placement and power allocation optimization. It discretizes the radar placement area into small grids, and then a sequential exhaustive enumeration geometric method and the water-filling power distribution algorithm are used to optimize variables, respectively. Different from [19], ref. [20] minimizes the total transmit power by the Lagrangian method and domain decompositions. Refs. [19,20] enhance the detection performance of the radar system; however, the antenna placement and power allocation in optimization processes are often optimized separately according to different objective functions, resulting in deviations from the global optimum.

For this reason, some collaborative methods may be suitable for solving such joint optimization problems. For instance, the combination of distributed MIMO radar nodes selection and power allocation based on target localization accuracy is investigated in ref. [21]. It utilizes the performance matrix as the single criterion for a two-step optimiza-

tion method and converts it into a second-order cone problem to solve. Further, ref. [22] studies the joint optimization problem of tracking multiple targets and it uses predicted conditional Cramér–Rao lower bound (PC-CRLB) as an optimization criterion for a two-step semidefinite-programming-based solution to solve this problem. Apart from the previous works, ref. [29] formulates the cost function by minimizing the sum of weighted PC-CRLB, integrating the subarray selection with power allocation optimization by a two-stage local search-based algorithm. More recently, ref. [30] develops a collaborative radar node selection and transmitter resource allocation algorithm for target tracking applications in multiple radar architectures. An efficient two-stage-based solution methodology that incorporates the interior point method and cyclic minimization framework makes it converge to the optimal solution.

1.2. Contributions

In light of the aforementioned literature, joint optimization has outstanding effectiveness in improving the radar system performance. However, few studies that concentrate on the problem of joint radar antenna placement and transmitter resource allocation (JAPPA) with the objective of target detection have been investigated. This gap promotes this research.

In the current paper, the JAPPA under a collaboratively unified objective function is investigated by considering radar detection performance optimization. Our primary contributions are summarized as follows.

1. We formulate the joint power allocation and antenna placement problem as an optimization model subject to the resource budget and area priority level. In the proposed JAPPA model, binary composite hypothesis testing is established to design the Neyman–Pearson (NP) detector for the whole surveillance area with the targets Radar Cross Section (RCS) obeying Rayleigh distribution. Compared to previous oversimplified works [19,20], the weighted NP-based logarithm likelihood ratio test (LRT) function is specified as the utility function that combines all optimization factors into a single objective function. In addition, we evaluate the average utility function values after changing the single stationary target’s position in the whole region to describe the global target detection performance of the radar network.
2. We propose an efficient JAPPA strategy that incorporates antenna placement with power allocation to optimize the target detection performance in the radar network. Different from the 0–1 programming in [21,31], we choose suitable antenna deployment positions in the regional grid points to establish the non-linear mixed integer programming problem. To devise computationally feasible methods for practical applications, a two-stage local-search-based algorithm is proposed to split the coupled joint optimization. Herein, it isolates integer programming from continuous variable optimization and provides equivalent performance while requiring less computing effort.
3. We develop a joint optimization closed-loop scheme for the joint antenna placement and power allocation optimization [30]. In our scheme, the optimal position results in the current cycle are used for guiding the power allocation. The detection performance will be further improved through this link, which renders a closed-loop scheme to repeat the iteration of transmitting and receiving antenna placement using the optimal power allocation scheme.

1.3. Organization

The remainder of the paper is organized as follows: Section 2 establishes the system model and NP-based detection model. Section 3 develops the optimization model and proposes an efficient solver. Based on the solver, a two-stage closed-loop method for resource allocation is built. Simulation results and contrast test data are presented in Section 4 to verify the effectiveness and superiority of the proposed method. Finally, Section 5 concludes the paper’s results and achievements.

Notations: For clarity, some notations used in this paper are listed as follows, and others will be explained when they first appear: The boldface is used for vectors \mathbf{s} (lower

case) and matrices \mathbf{A} (upper case). Superscript $(\cdot)^T$ denotes the transpose operators. $\mathcal{N}(a, b)$ represents the Gaussian normal distribution where the mean is a , and the variance is b . $P_{T,k}^m$ indicates the allocated power to the m -th transmitting antenna in the k -th iteration loop. Moreover, $\mathbf{L}_{T,k}$ and $\mathbf{L}_{R,k}$ denote the transmitting antenna and receiving antenna locations in the k -th iteration loop, respectively.

2. System Model and Detection Formulation

2.1. Signal Model

Note that the detection performance of a distributed MIMO radar is an essential indicator for evaluating radar network surveillance performance. This paper discusses the joint antenna placement and optimal power allocation method in a two-dimensional Cartesian coordinate system. We consider a distributed MIMO radar network with M transmitters and N receivers. The m -th transmitter is positioned at the coordinate (x_T^m, y_T^m) for $m = 1, \dots, M$, the n -th receiver is positioned at the coordinate (x_R^n, y_R^n) for $n = 1, \dots, N$, respectively. Besides, the position of the target is (x_t, y_t) . Figure 1 illustrates the considered distributed MIMO radar network configuration sketch with $M = N = 3$.

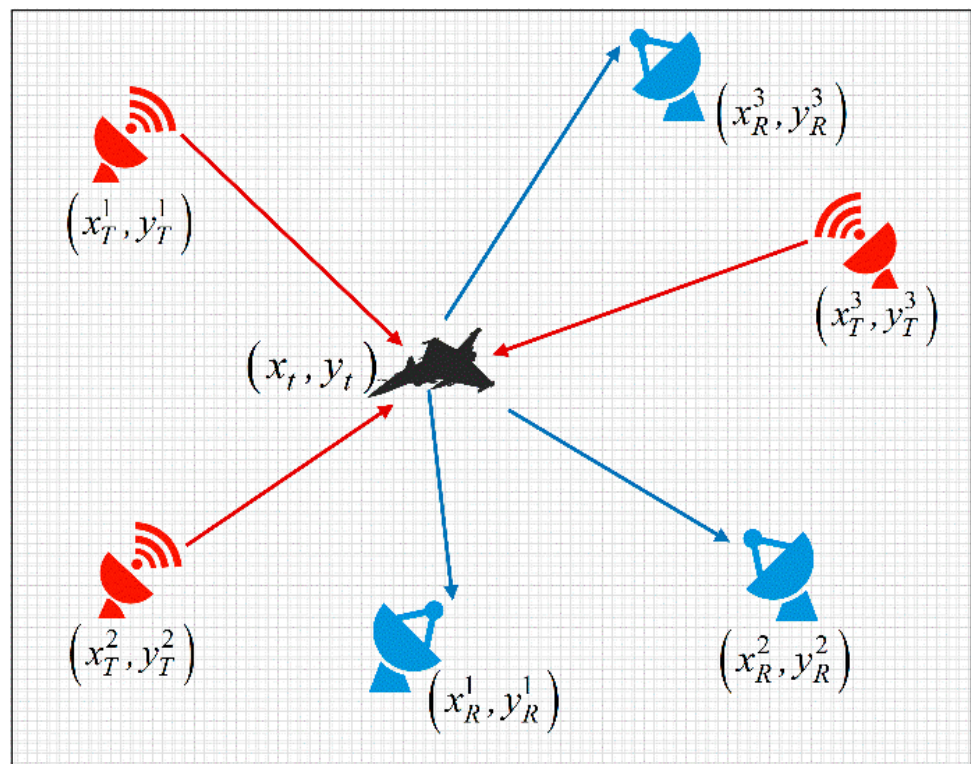


Figure 1. System configuration for distributed MIMO radar network.

The MIMO radar transmitting array elements simultaneously transmit a set of normalized orthogonal signals to the far-field target, and the precoding waveform vector satisfies

$$\int_{-\infty}^{\infty} s_m(t) s_{m'}^H(t - \tau) dt = \begin{cases} 1 & \text{for } m = m', \tau = 0 \\ 0 & \text{for } \text{otherwise} \end{cases} \quad (1)$$

where $s_m(t)$ denotes the corresponding baseband signal, f_c is the signal carrier frequency, and τ_m is the duration time of the m -th signal.

As such, the baseband signal transmitted from the m -th transmitting antenna to the n -th receiving antenna can be expressed as:

$$\mathbf{r}_{nm} = \sqrt{\mathbf{P}_{Tm} \mathbf{L}_{nm}} \cdot \mathbf{C}_{nm} \cdot \mathbf{s}_m(t - \tau_{nm}) \cdot e^{j2\pi f_{d, nm} t} + \mathbf{n}_n(t) \quad (2)$$

$$\sqrt{\mathbf{P}_{Tm}\mathbf{L}_{nm}} = \begin{bmatrix} \sqrt{P_{T1}L_{11}} & \sqrt{P_{T2}L_{12}} & \cdots & \sqrt{P_{TM}L_{1M}} \\ \vdots & \vdots & \vdots & \vdots \\ \sqrt{P_{TN}L_{N1}} & \sqrt{P_{T2}L_{N2}} & \cdots & \sqrt{P_{TM}L_{NM}} \end{bmatrix}_{N \times M} \tag{3}$$

$$\mathbf{C}_{nm} = \begin{bmatrix} c_{11} & c_{12} & \cdots & c_{1N} \\ \vdots & \vdots & \vdots & \vdots \\ c_{M1} & c_{M2} & \cdots & c_{MN} \end{bmatrix}_{M \times N} \tag{4}$$

where \mathbf{L}_{nm} is the propagation that includes antenna gains, \mathbf{P}_{Tm} is the radar transmit power, \mathbf{C}_{nm} is scattering amplitude that includes any unknown oscillator phase terms, \mathbf{s}_m is the signal transmitted by the m -th transmitting antenna, τ_{nm} is the time-delay, $f_{d,nm}$ is the Doppler shift caused by target movement. Moreover, $\mathbf{n}_n(t)$ presents the additive complex white Gaussian noise vector at the receiver.

With the assumptions above, the baseband signal received by the n -th receiving antenna of the distributed MIMO radar can be written as:

$$r_n(t) = \sum_{m=1}^M r_{mn}(t) = \sum_{m=1}^M E_{nm} \cdot c_{nm} \cdot s_m(t - \tau_{nm}) \cdot e^{j2\pi f_{d,nm}t} + n_n(t) \tag{5}$$

where $n_n(t)$ is the zero-mean white complex noise at n -th receiver, and

$$E_{nm} \in \mathbf{E}_n = [\sqrt{P_{T1}L_{n1}}, \sqrt{P_{T2}L_{n2}}, \dots, \sqrt{P_{TM}L_{nM}}]_{1 \times M} \tag{6}$$

$$c_{nm} \in \mathbf{C}_n = [c_{n1}, c_{n2}, \dots, c_{nM}]_{1 \times M} \tag{7}$$

2.2. Neyman–Pearson Detection Model

The decision of target existence in a distributed MIMO radar network is made without any prior probability. Therefore, the NP criterion is suitable for radar detection [31]. Herein, we develop the NP detector for a distributed MIMO radar network in this section, seeking the optimal antenna position and power allocation scheme.

The NP detector establishes the LRT and compares it with the threshold η specified by the P_{fa} . It yields two likelihood hypotheses, as shown in (8): the null hypothesis (signal-absence) \mathcal{H}_0 and the alternative hypothesis (signal-presence) \mathcal{H}_1 . It is noticeable that distributed MIMO radar network detection hypotheses are given for each receiver.

$$\begin{cases} \mathcal{H}_0 : & r_n = n_n(t) \\ \mathcal{H}_1 : & r_n = \sum_{m=1}^M E_{nm} \cdot c_{nm} \cdot s_m(t - \tau_{nm})e^{j2\pi f_{d,nm}t} + n_n(t) \end{cases}, n = 1, \dots, N \tag{8}$$

In this paper, the target comprises multiple randomly distributed independent scatterers of roughly equal areas. Hence, the target RCS is assumed under the Rayleigh scattering model, and the Swerling I model is defined as [32]:

$$f_{\sigma_t} = \frac{x}{\sigma_0^2} e^{-\frac{x^2}{2\sigma_0^2}} \tag{9}$$

where σ_0^2 is the average RCS of the object. According to the free space propagation loss equation analysis, the amplitude of the signal received by the n -th receiver can be cast as (10) [32].

$$\alpha_{nm} = \frac{\sigma_t}{R_{mt}R_{tn}} \sqrt{\frac{P_{Tm}G_tG_rI_p\lambda^2}{(4\pi)^3L_cL_r}} \tag{10}$$

where P_{Tm} is the transmitted power, σ_t is RCS of the target, G_t and G_r are the transmitter and receiver gains, respectively, I_p is the receiving processing gain, λ is radar signal wavelength, L_c and L_r are the scattering loss and receiving loss, respectively. R_{mt} and R_{tn} are the

distance between the m -th transmitter to target and target to the n -th receiver. Due to the widely separated antennas, different α_{nm} s are regarded as independent and the echo amplitude is proportional to the RCS, resulting in a Rayleigh distribution for amplitude α_{nm} . Substituting (10) in (9), it can be deduced that

$$f_{\alpha_{nm}} = \frac{x}{\sigma_{nm}^2} e^{-\frac{x^2}{2\sigma_{nm}^2}} \quad (11)$$

where

$$\sigma_{nm}^2 = \frac{P_{Tm} G_r G_t I_p \sigma_0^2 \lambda^2}{(4\pi)^3 R_{mt}^2 R_{tn}^2 L_c L_r} \quad (12)$$

Therefore, we have

$$\alpha_{nm} = E_{nm} \cdot c_{nm} \cdot e^{j2\pi f_{d, nm} t} \quad (13)$$

The received signal r_n can be redefined as

$$r_n = \sum_{m=1}^M \alpha_{nm} \cdot s_m(t - \tau_{nm}) e^{j2\pi f_{d, nm} t} + n_n(t) \quad (14)$$

Then, a likelihood ratio detection session is performed after the echo signal passes through the filter bank and sampler. Thus, a binary hypothesis can be expressed as follows:

$$y_n = \begin{cases} \sum_{m=1}^M a_{nm} \cdot s_m(t - \tau_{nm}) + n_n, & \mathcal{H}_1 \\ n_n, & \mathcal{H}_0 \end{cases} \quad (15)$$

where $\mathbf{y}_n = [y_1, y_1, \dots, y_n]^T$ represents the received signal test data vector, s_m is the sample version signal to be detected, n_n is the noise in the test. In addition, we assume the noise model is a Gaussian distributed model that satisfies $n_n \sim \mathcal{N}(0, \sigma^2)$, then the joint probability density function (PDF) of the test data \mathbf{y}_n is defined as

$$\begin{cases} f_{\mathbf{Y}_n}(\mathbf{y}_n | \mathcal{H}_0) \sim \mathcal{N}(0, \sigma^2 \mathbf{I}_N) \\ f_{\mathbf{Y}_n}(\mathbf{y}_n | \mathcal{H}_1, \alpha_{nm}) \sim \mathcal{N}(\mathbf{r}_{0n}, \sigma^2 \mathbf{I}_N) \end{cases} \quad (16)$$

In the above equation, $\mathbf{r}_{0n} \triangleq \sum_{m=1}^M a_{nm} \cdot \mathbf{s}_m(t - \tau_{nm})$, and $\sigma^2 \mathbf{I}_N$ denotes the noise variance and identity matrix $\mathbf{I}_N = \text{diag}(1, \dots, 1)_{1 \times N}$. Then, the LRT for the NP detector is usually given as follows [33]

$$L(\mathbf{y}_n) = \frac{f_{\mathbf{Y}_n}(\mathbf{y}_n | \mathcal{H}_1)}{f_{\mathbf{Y}_n}(\mathbf{y}_n | \mathcal{H}_0)} \underset{\mathcal{H}_0}{\overset{\mathcal{H}_1}{>}} \eta \quad (17)$$

where η is a threshold determined by P_{fa} . Based on this derivation, hypothesis \mathcal{H}_0 and \mathcal{H}_1 probability density function models are, respectively, defined as:

$$f_{\mathbf{Y}_n}(\mathbf{y}_n | \mathcal{H}_0) = \prod_{n=1}^N \frac{1}{\sqrt{2\pi\sigma^2}} \exp\left\{-\frac{1}{2} \left(\frac{\|\mathbf{y}_n\|^2}{\sigma^2}\right)\right\} \quad (18)$$

$$f_{\mathbf{Y}_n}(\mathbf{y}_n | \mathcal{H}_1, \alpha_{mn}) = \prod_{n=1}^N \frac{1}{\sqrt{2\pi\sigma^2}} \exp\left\{-\frac{1}{2} \left(\frac{\|\mathbf{y}_n - \mathbf{r}_{0n}\|^2}{\sigma^2}\right)\right\} \quad (19)$$

According to the specific PDF in (16) and substituting from (11), (19) can be derived as:

$$\begin{aligned}
f_{\mathbf{Y}_n}(\mathbf{y}_n|\mathcal{H}_1) &= \int_0^\infty \cdots \int_0^\infty f_{\mathbf{Y}_n}(\mathbf{y}_n|\mathcal{H}_1, \alpha_{nm}) \prod_{m=1}^M \prod_{n=1}^N f_{\alpha_{nm}}(\alpha_{nm}) d\alpha_{nm} \\
&= \int_0^\infty \cdots \int_0^\infty \left\{ \frac{1}{(t-\tau_{nm})^{N/2}} \exp \sum_{n=1}^N \left\{ -\frac{1}{2} \left(\frac{\|\mathbf{y}_n\|^2 - 2\mathbf{y}_n^T \cdot \mathbf{r}_{0n} + \|\mathbf{r}_{0n}\|^2}{\sigma^2} \right) \right\} \right\} \prod_{m=1}^M \prod_{n=1}^N f_{\alpha_{nm}}(\alpha_{nm}) d\alpha_{nm}
\end{aligned} \quad (20)$$

Based on the previous Formulas (1) and (10)–(14), we can make a substitution due to the orthogonality of the distributed radar signals that

$$\|\mathbf{r}_{0n}\|^2 = \mathbf{r}_{0n}^T \cdot \mathbf{r}_{0n} = \sum_{m=1}^M \sum_{m'=1}^M \alpha_{nm} \cdot \mathbf{s}^T(t - \tau_{nm}) \cdot \alpha_{nm} \cdot \mathbf{s}(t - \tau_{nm}) = \sum_{m=1}^M \alpha_{nm}^2 \quad (21)$$

and

$$\|\mathbf{y}_n\|^2 = \mathbf{y}_n^T \cdot \mathbf{y}_n = \frac{1}{M} \sum_{m=1}^M \|\mathbf{y}_n\|^2 \quad (22)$$

$$2\mathbf{y}_n^T \cdot \mathbf{r}_{0n} = 2\alpha_{nm} \sum_{m=1}^M \mathbf{y}_n^T \cdot \mathbf{s}_m(t - \tau_{nm}) \quad (23)$$

Substituting (21)–(23) into (20), it is easy to find that

$$\begin{aligned}
f_{\mathbf{Y}_n}(\mathbf{y}_n|\mathcal{H}_1) &= \int_0^\infty \cdots \int_0^\infty \left\{ \frac{1}{(2\pi\sigma^2)^{N/2}} \exp \left\{ -\frac{1}{2} \left(\frac{\frac{1}{M} \sum_{n=1}^N \sum_{m=1}^M \|\mathbf{y}_n\|^2 - 2\alpha_{nm} \mathbf{y}_n^T \cdot \mathbf{s}_m(t - \tau_{nm}) + \alpha_{nm}^2}{\sigma^2} \right) \right\} \right\} \times \prod_{m=1}^M \prod_{n=1}^N f_{\alpha_{nm}}(\alpha_{nm}) d\alpha_{nm} \\
&= \frac{1}{(2\pi\sigma^2)^{N/2}} \prod_{m=1}^M \prod_{n=1}^N \left(\int_0^\infty \exp \left(\frac{\sum_{n=1}^N \sum_{m=1}^M \frac{1}{M} \|\mathbf{y}_n\|^2 - 2\alpha_{nm} \mathbf{y}_n^T \cdot \mathbf{s}_m(t - \tau_{nm}) + \alpha_{nm}^2}{-2\sigma^2} \right) f_{\alpha_{nm}}(\alpha_{nm}) d\alpha_{nm} \right) \\
&= \frac{1}{(2\pi\sigma^2)^{N/2}} \prod_{m=1}^M \prod_{n=1}^N K_{nm}
\end{aligned} \quad (24)$$

where

$$\begin{aligned}
K_{nm} &= \int_0^\infty \exp \left(\frac{\frac{1}{M} \|\mathbf{y}_n\|^2 - 2x \cdot \mathbf{y}_n^T \cdot \mathbf{s}_m(t - \tau_{nm}) + \alpha_{nm}^2}{-2\sigma^2} \right) f_{\alpha_{nm}}(\alpha_{nm}) d\alpha_{nm} \\
&= \int_0^\infty \exp \left(\frac{\frac{1}{M} \|\mathbf{y}_n\|^2 - 2x \cdot \mathbf{y}_n^T \cdot \mathbf{s}_m(t - \tau_{nm}) + x^2}{-2\sigma^2} \right) \frac{x}{\sigma_{nm}^2} e^{-\frac{x^2}{2\sigma_{nm}^2}} dx \\
&= \frac{1}{\sigma_{nm}^2} \exp \left(-\frac{\|\mathbf{y}_n\|^2}{2M\sigma^2} \right) \int_0^\infty x \exp \left(\frac{x \cdot \mathbf{y}_n^T \cdot \mathbf{s}_m(t - \tau_{nm})}{\sigma^2} - x^2 \left(\frac{1}{2\sigma_{nm}^2} + \frac{1}{2\sigma^2} \right) \right) dx
\end{aligned} \quad (25)$$

Substituting $\frac{1}{2\sigma_{nm}^2} + \frac{1}{2\sigma^2} = b^2$ and $\frac{\mathbf{y}_n^T \cdot \mathbf{s}_m(t - \tau_{nm})}{\sigma^2} = c$ into (25), then, K_{nm} can be rewritten as

$$\begin{aligned}
K_{nm} &= \frac{1}{\sigma_{nm}^2} \exp \left(-\frac{\|\mathbf{y}_n\|^2}{2M\sigma^2} \right) \int_0^\infty x \exp(xc - x^2b^2) dx \\
&= \frac{1}{2b^2\sigma_{nm}^2} \exp \left(\frac{\|\mathbf{y}_n\|^2}{-2M\sigma^2} \right) \left(1 + \frac{c}{b} \cdot \exp \left(\frac{c^2}{4b^2} \right) \cdot \int_{-\frac{c}{2b}}^\infty \exp(-p^2) dp \right)
\end{aligned} \quad (26)$$

where $p = bx - \frac{c}{2b}$. Therefore, the corresponding LRT function can be calculated as:

$$L(\mathbf{y}_n) = \frac{f_{\mathbf{Y}_n}(\mathbf{y}_n|\mathcal{H}_1)}{f_{\mathbf{Y}_n}(\mathbf{y}_n|\mathcal{H}_0)} = \prod_{m=1}^M \prod_{n=1}^N \frac{1}{1 + \frac{\sigma_{nm}^2}{\sigma^2}} \left(1 + \sqrt{\pi} \frac{c}{b} \exp \left(\frac{c^2}{4b^2} \right) \cdot \int_{-\frac{c}{2b}}^\infty \exp(-p^2) dp \right) \quad (27)$$

To alleviate the detector calculation complexity, the radar network high-SNR condition, $\sigma_{nm}^2 \gg \sigma^2$, is typically utilized to simplify the formula. Thus, b^2 can be redefined as:

$$b^2 \triangleq \frac{1}{2\sigma_{nm}^2} + \frac{1}{2\sigma^2} = \frac{1}{2\sigma^2} \tag{28}$$

Using $\int_{-\frac{c}{2b}}^{\infty} \exp(-p^2) dp \approx 1 - \frac{1}{\sqrt{\pi}(c/b)} \cdot \exp(-c^2/4b^2)$, $\sigma_{nm}/\sigma \gg 1$, (27) can be rewritten as

$$\begin{aligned} L(\mathbf{y}_n) &= \prod_{m=1}^M \prod_{n=1}^N \frac{1}{1 + \frac{\sigma_{nm}^2}{\sigma^2}} \left(1 + \sqrt{\pi} \frac{c}{b} \exp\left(\frac{c^2}{4b^2}\right) \cdot \int_{-\frac{c}{2b}}^{\infty} \exp(-p^2) dp \right) \\ &= \prod_{m=1}^M \prod_{n=1}^N \left(\frac{\sqrt{\pi} \frac{c}{b} \cdot \exp\left(\frac{c^2}{4b^2}\right)}{1 + \frac{\sigma_{nm}^2}{\sigma^2}} \right) \end{aligned} \tag{29}$$

Herein, we have tests statistics of the NP detector,

$$\mathbb{T}_{\text{MIMO}} = \prod_{m=1}^M \prod_{n=1}^N \left(\frac{\sqrt{\pi} \frac{c}{b} \cdot \exp\left(\frac{c^2}{4b^2}\right)}{1 + \frac{\sigma_{nm}^2}{\sigma^2}} \right) \begin{matrix} > \eta \\ < \eta \end{matrix} \tag{30}$$

where

$$\frac{c}{b} = \frac{\mathbf{y}_n^T \cdot \mathbf{s}_m(t - \tau_{nm})}{\sqrt{\frac{1}{2\sigma^2}}} = \sqrt{2} \cdot \frac{\mathbf{y}_n^T \cdot \mathbf{s}_m(t - \tau_{nm})}{\sigma} = \sqrt{2} \cdot \frac{E_{nm} \cdot c_{nm}}{\sigma} \tag{31}$$

Since the test statistic \mathbb{T}_{MIMO} is always positive, we can substitute (30) into (31) and take the logarithm of the two ends to obtain the logarithmic LRT function (log-LRT) shown in (32). Finally, $\text{Ln}(\mathbb{T}_{\text{MIMO}})$ can be compared with the new threshold η' which equals $\text{Ln}(\eta)$.

$$\text{Ln}(\mathbb{T}_{\text{MIMO}}) = \sum_{m=1}^M \sum_{n=1}^N \left[\text{Ln} \left(\sqrt{2\pi} \cdot \frac{E_{nm} \cdot c_{nm}}{\sigma} \cdot \exp \left(\frac{(E_{nm} \cdot c_{nm})^2}{2\sigma^2} \right) \right) - \text{Ln} \left(1 + \frac{\sigma_{nm}^2}{\sigma^2} \right) \right] \begin{matrix} > \eta' \\ < \eta' \end{matrix} \tag{32}$$

Remark: The simplification of expression (28) can be performed only under high-SNR conditions. As for the case of low-SNR conditions, it will be considered in our future works, which will further enrich the radar system application scenarios in the future.

3. Antenna Placement and Power Allocation Strategy

Aiming at solving the JAPPA problem, we proposed an efficient JAPPA strategy for target detection by using a distributed MIMO radar system. First, the combat area needs to be discretized into grid areas to optimize antenna placement using the numerical method. Then, as shown in the blue dashed box, the antenna location deployment and transmitter power allocation can be optimized by the strategy based on the NP criterion. Finally, the jointly optimal solution can be obtained by a closed-loop iterative approach, shown in red. The whole method structure is illustrated in Figure 2.

3.1. Optimization Formulation

Mathematically, the JAPPA strategy incorporates the antenna placement with power allocation to achieve optimal target detection performance based on the regional characteristics and predetermined power budget. The NP-based detection criterion deduced in Section 3 is appropriate to construct the objective function.

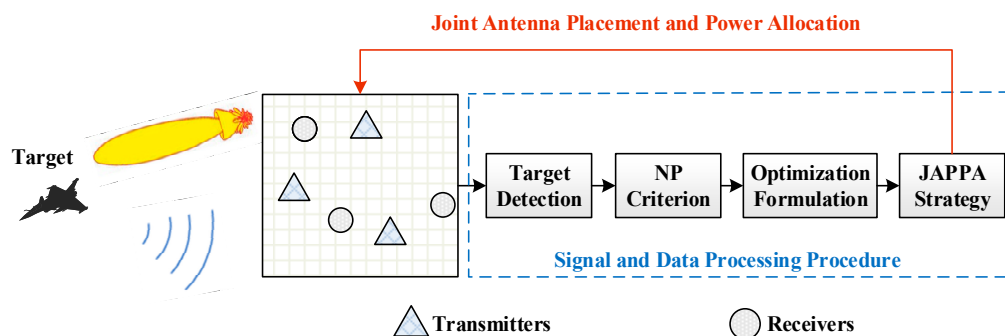


Figure 2. Illustration of the proposed JAPPA method.

First, we define the following vectors: the transmitter antenna position vector is $\mathbf{L}_{Tk} = [L_{T,k}^1, \dots, L_{T,k}^m, \dots, L_{T,k}^M]^T$, $L_{T,k}^m = (x_{T,k}^m, y_{T,k}^m)$. The receiver antenna position vector is $\mathbf{L}_{Rk} = [L_{R,k}^1, \dots, L_{R,k}^n, \dots, L_{R,k}^N]^T$, $L_{R,k}^n = (x_{R,k}^n, y_{R,k}^n)$. The transmitter power allocation vector is $\mathbf{P}_{Tk} = [P_{T1,k}, \dots, P_{Tm,k}, \dots, P_{TM,k}]^T$. Then, the log-LRT can be rewritten as

$$\text{Ln}\{\mathbb{T}_{\text{MIMO}}(\mathbf{L}_{Tk}, \mathbf{L}_{Rk}, \mathbf{P}_{Tk})\} = \sum_{m=1}^M \sum_{n=1}^N \left[\text{Ln} \left(\sqrt{2\pi} \cdot \frac{E_{nm} \cdot c_{nm}}{\sigma} \cdot \exp \left(\frac{(E_{nm} \cdot c_{nm})^2}{2\sigma^2} \right) \right) - \text{Ln} \left(1 + \frac{\sigma_{nm}^2}{\sigma^2} \right) \right] \underset{\mathcal{H}_0}{\overset{\mathcal{H}_1}{>}} \eta' \quad (33)$$

Considering a realistic confrontation, we set up an area with a priority level using the historical statistic of non-cooperative targets (enemy targets) violations. The position with a higher threat level has higher priority and higher detection probability requirements, and vice versa. In this way, the priority level is utilized as a weighting coefficient multiplying with the NP-based log-LRT at each location. Therefore, it is preferred to use the sum of weighted NP-based log-LRT as the objective function.

$$\mathbb{F}(\mathbf{L}_{Tk}, \mathbf{L}_{Rk}, \mathbf{P}_{Tk}) = \mathbb{E}\{\zeta_q [\mathbb{T}_{\text{MIMO}}(\mathbf{L}_{Tk}, \mathbf{L}_{Rk}, \mathbf{P}_{Tk})]\} \quad (34)$$

where $\mathbb{E}\{\cdot\}$ is expectation operation, \mathbb{T}_{MIMO} is the NP-based log-LRT statistic. ζ_q is the priority level coefficient, which can be determined by the comprehensive consideration of the military objective location, operational missions, and other parameters. Although the numerical computation of ζ_q is beyond the scope of this paper, just for simplicity, we pre-define the priority levels for each regional grid point directly in the simulation.

Many constraints should be taken into account. Firstly, the optimal strategy for the radar network should be subject to acceptable target detection performance.

$$\text{Ln}\{\mathbb{T}_{\text{MIMO}}(\mathbf{L}_{Tk}, \mathbf{L}_{Rk}, \mathbf{P}_{Tk})\} > \eta' \quad (35)$$

Then, the sum of the transmitters' consumption power is bound by a power budget P_{TOTAL} .

$$\mathbf{1}_M^T \mathbf{P}_{Tk} \leq P_{\text{TOTAL}} \quad (36)$$

where $\mathbf{1}_M^T = [1, 1, \dots, 1]_{1 \times M}$. Next, each transmitter sets the minimum and maximum power values as the constraints [34].

$$\begin{cases} P_{T_{kmin}} \leq P_{T_{m,k}} \\ P_{T_{m,k}} \leq P_{T_{kmax}} \end{cases} \quad (37)$$

Therefore, the JAPPA optimization model can be formulated as

$$\begin{aligned}
 & \mathcal{P} : \max \mathbb{F}(\mathbf{L}_{Tk}, \mathbf{L}_{Rk}, \mathbf{P}_{Tk}) \\
 \text{s.t. } & \mathcal{C1}: \mathbf{1}_M^T \mathbf{P}_{Tk} \leq P_{TOTAL} \\
 & \mathcal{C2}: 0 \leq P_{Tkmin} \leq P_{Tm,k}, \quad \forall m \in \mathcal{M} : \{1, \dots, M\} \\
 & \mathcal{C3}: 0 \leq P_{Tm,k} \leq P_{Tkmax}, \quad \forall m \in \mathcal{M} : \{1, \dots, M\} \\
 & \mathcal{C4}: x_T^m, y_T^m \in \mathcal{NET}, \quad \forall m \in \mathcal{M} : \{1, \dots, M\} \\
 & \mathcal{C5}: x_R^n, y_R^n \in \mathcal{NET}, \quad \forall n \in \mathcal{N} : \{1, \dots, N\}
 \end{aligned} \tag{38}$$

where \mathcal{M} and \mathcal{N} represent the sets of antenna labels, and \mathcal{NET} represents the antenna candidate points set. Besides, $\mathcal{C1}$ is the total power consumption constraint, $\mathcal{C2}$ and $\mathcal{C3}$ represents the upper and lower power bounds for each transmitter antenna, respectively. $\mathcal{C4}$ and $\mathcal{C5}$ ensure the antennas are placed on the coordinate grid point.

3.2. Solution Technique

Due to the presence of the radar transceiver antenna term \mathbf{L}_{Tk} and \mathbf{L}_{Rk} in the objective function, (38) is essentially a non-convex non-linear mixed integer programming problem, and problem-solving is non-deterministic polynomial-time hard. A direct method is to partition the discrete coordinate position variables and continuous power variables to search for a solution [22,35].

Here, we propose a novel algorithm based on a two-stage local search, a mixed-integer global optimization algorithm based on greedy take-away and Lagrange. The discrete variable coordinates and the continuous variables are divided using the cutting plane to obtain the integer variable linear approximation of the non-linear programming model. Once the value of the integer variable is determined, the corresponding continuous variable is solved by the Lagrangian function [36]. Finally, integer variables and continuous variables together constitute a feasible solution to the original model. The steps are shown as follows.

3.2.1. Local Search for Antenna Placement

In this case, we define the power of each transmitter as uniformly allocated, i.e., $P_{T,average} = P_{TOTAL} / M$. The transmitting and receiving antenna deployment at the points from the grid area are known to be NP hard. Simultaneous completion of transmitting and receiving antennas is an arduous computational task; although the exhaustive search method is feasible, the computational effort grows exponentially [27]. Therefore, it is necessary to separate the two antenna arrangements, and the optimization equations for transmitter and receiver antenna placement are, respectively, given below.

$$\begin{aligned}
 \text{Transmitter : } & \mathcal{P} : \max \mathbb{F}(\mathbf{L}_{T,k+1}, \mathbf{L}_{R,k}, \mathbf{P}_{T,average}) \\
 \text{s.t. } & \mathcal{C1} : x_{T,k+1}^m, y_{T,k+1}^m \in \mathcal{NET}, \quad \forall m \in \mathcal{M} : \{1, \dots, M\} \\
 & \mathcal{C2} : x_{R,k'}^n, y_{R,k'}^n \in \mathcal{NET}, \quad \forall n \in \mathcal{N} : \{1, \dots, N\}
 \end{aligned} \tag{39}$$

$$\begin{aligned}
 \text{Receiver : } & \mathcal{P} : \max \mathbb{F}(\mathbf{L}_{T,k+1}, \mathbf{L}_{R,k+1}, \mathbf{P}_{T,average}) \\
 \text{s.t. } & \mathcal{C1} : x_{T,k+1}^m, y_{T,k+1}^m \in \mathcal{NET}, \quad \forall m \in \mathcal{M} : \{1, \dots, M\} \\
 & \mathcal{C2} : x_{R,k+1}^n, y_{R,k+1}^n \in \mathcal{NET}, \quad \forall n \in \mathcal{N} : \{1, \dots, N\}
 \end{aligned} \tag{40}$$

Initially, a dense uniformed grid with different priority levels over the antenna placement area is assumed, each of the grid points of which serves as a potential antenna placement location. Based on this structure, we propose a site selection algorithm based on a two-stage greedy dropping heuristic to optimize the antenna positions of the transmitter and receiver successively. The purpose is to choose M positions to place the transmitting antennas and then select N positions to place the receiving antennas from the candidate positions to optimize the objective function. Meanwhile, a taboo list has been set up to accelerate the convergence speed. The summary of this algorithm is given in Algorithm 1 (Local search for antenna placement).

Algorithm 1: Two-stage greedy dropping heuristic local search for antenna placement**Input:** $M, N, \mathcal{NET}, \zeta_q$ **Output:** optimal $\mathbf{L}_{T,k} = [L_{T,k}^1, \dots, L_{T,k}^m, \dots, L_{T,k}^M]^T$ and $\mathbf{L}_{R,k} = [L_{R,k}^1, \dots, L_{R,k}^n, \dots, L_{R,k}^N]^T$

```

1 Initialize  $k = 1, q = 1, L_{T,1}^1, \dots, L_{T,1}^M$  and  $L_{R,1}^1, \dots, L_{R,1}^N$ ;
2 double  $Temp_{0,1} = Temp_{1,0} = 0, \varepsilon = 1e - 6$ ;
3 while  $\mathbb{F}(\mathbf{L}_{T,k}, \mathbf{L}_{R,q}, \mathbf{P}_{T,average}) - Temp_{k-1,q} \geq \varepsilon$  do
4   Replaces  $Temp_{k,q} = \mathbb{F}(\mathbf{L}_{T,k}, \mathbf{L}_{R,q}, \mathbf{P}_{T,average})$ 
5   Recombines  $\mathbf{L}_{T,k}$ : substitute  $L_{T,k}^m$  with a new coordinate  $L, L \notin \mathbf{L}_{T,k} \cup \dots \cup \mathbf{L}_{T,0}$ 
6   if  $\mathbb{F}(\mathbf{L}'_{T,k}, \mathbf{L}_{R,q}, \mathbf{P}_{T,average}) \geq Temp_{q,k}$  then
7      $\mathbf{L}_{T,k+1} = \mathbf{L}'_{T,k}$ 
8     Removes the  $L$  from the set of candidate points
9   end if
10   $k = k + 1$ 
11 end while
12 while  $\mathbb{F}(\mathbf{L}_{T,k}, \mathbf{L}_{R,q}, \mathbf{P}_{T,average}) - Temp_{k,q-1} \geq \varepsilon$  do
13   Replaces  $Temp_{k,q} = \mathbb{F}(\mathbf{L}_{T,k}, \mathbf{L}_{R,q}, \mathbf{P}_{T,average})$ 
14   Recombines  $\mathbf{L}_{R,q}$ : substitute  $L_{R,q}^n$  with a new coordinate  $L, L \notin \mathbf{L}_{R,k} \cup \dots \cup \mathbf{L}_{R,0}$ 
15   if  $\mathbb{F}(\mathbf{L}_{T,k}, \mathbf{L}'_{R,q}, \mathbf{P}_{T,average}) \geq Temp_{k,q}$  then
16      $\mathbf{L}_{R,q} = \mathbf{L}'_{R,q}$ 
17     Removes the  $L$  from the set of candidate points
18   end if
19    $q = q + 1$ 
20 end while
21 return  $\mathbf{L}_{T,k+1}, \mathbf{L}_{R,k+1}$ 

```

3.2.2. Local-Search-Based Lagrange-KKT for Power Allocation

The premise of power allocation is antenna placement; therefore, the optimization model can be given by

$$\begin{aligned}
 \mathcal{P} : & \max \mathbb{F}(\mathbf{P}_{T,k+1}) \\
 \text{C1:} & \mathbf{1}_M^T \mathbf{P}_{T,k+1} = P_{TOTAL} \\
 \text{C2:} & 0 \leq P_{Tmin} \leq P_{T,k}^m \quad \forall m \in \mathcal{M} : \{1, \dots, M\} \\
 \text{C3:} & 0 \leq P_{T,k}^m \leq P_{Tmax}, \quad \forall m \in \mathcal{M} : \{1, \dots, M\}
 \end{aligned} \tag{41}$$

where the only variable is the transmitter power vector $\mathbf{P}_{T,k+1}$ and the problem has been transformed into a univariate optimization model. Thus, the corresponding continuous variable power values can be determined by solving the sub-problems (41). Herein, a Lagrangian multiplier method and the Karush–Kuhn–Tucker (KKT) condition are used to solve the optimal power allocation among transmitters [37], and the Lagrangian function is written in the following

$$\mathcal{L} = \mathbb{F}(\mathbf{P}_{T,k+1}) - \lambda_1(P_{Tmin} - P_{Tm,k+1}) - \lambda_2(P_{Tm,k+1} - P_{Tmax}) - \mu \left(\sum_{m=1}^M P_{Tm,k+1} - P_{TOTAL} \right) \tag{42}$$

Appendix A proves that (41) is a non-linear convex optimization problem and concludes that the approximate task utility function is unimodal [38]. From this, the optimal power allocation strategy can be obtained, and we have

$$\nabla_{\mathbf{P}_{T,k+1}} \mathcal{L} \left(\mathbf{P}_{T,k+1}, \bar{\lambda}, \bar{\mu} \right) = 0 \tag{43}$$

where $\mathbf{P}_{T,k+1}$ is the local optimum of the problem (41), $\lambda = [\lambda_1, \lambda_2]$ and $\bar{\mu}$ are multiplier vectors; the KKT conditions are formulated as

$$\begin{cases} \nabla_{P_{T,k+1}} \mathcal{L} = \sum_{n=1}^N \left(\frac{1}{2P_{Tm,k+1}} + \frac{L_{nm}c_{nm}^2}{2\sigma^2} - \frac{L_{nm}c_{nm}^2}{\sigma^2 + L_{nm}c_{nm}^2 P_{Tm,k+1}} \right) + \lambda_1 - \lambda_2 - \mu = 0 \\ \nabla_{\lambda_1} \mathcal{L} = P_{Tmin} - P_{Tm,k+1} = 0 \\ \nabla_{\lambda_2} \mathcal{L} = P_{Tm,k+1} - P_{Tmax} = 0 \\ \nabla_{\mu} \mathcal{L} = P_{TOTAL} - \sum_{m=1}^M P_{Tm,k+1} = 0 \\ \lambda \geq 0 \end{cases} \quad (44)$$

Considering $\sigma^2 \ll P_{T,k+1}^m L_{mn} C_{mn}^2$ and all transmitting antennas have to operate, i.e., the inequality constraint cannot fetch an equal sign. Therefore, we simplify the constraint conditions that $\lambda_1 = \lambda_2 = 0$. The optimal transmitter power allocation strategy can be calculated as follows

$$\begin{cases} P_{T,k+1}^m = \frac{N}{2 \left(-\mu + \sum_{n=1}^N \frac{L_{nm}c_{nm}^2}{2\sigma^2} \right)} \\ \sum_{m=1}^M P_{Tm,k+1} = P_{TOTAL} \end{cases} \quad (45)$$

According to the properties of the convex function, the local optimum \mathbf{P}_T satisfying the KKT condition is the global optimum of (42), which is the optimal transmitter power allocation scheme. At this time, we have obtained the optimal transmitter power allocation scheme corresponding to the integer variable $(\mathbf{L}_{T,k+1}, \mathbf{L}_{R,k+1})$ that maximizes the target detection capability of the MIMO radar network based on the existing antenna deployment.

3.3. Closed-Loop Resource Allocation Scheme

Further on, we exploit the previous results in the last optimization cycle as the feedback information to implement joint antenna placement and power allocation optimization in distributed MIMO radar networks by successive optimization. Overall, we iteratively repeat transmitting and receiving antenna placement and power allocation. In such an operation, first, the updated power allocation scheme is used to obtain the optimal antenna placement scheme. Then, the placement scheme is employed to repeat the power allocation optimization. Finally, the JAPPA strategy incorporates the prior information to achieve the optimal antenna placement and power allocation, which results in superior detection performance in the next round of the period.

In this paper, we combine the idea of cycle minimization (CM) to separate coordinate deployment variables and power variables for cyclic optimization [29,30]. Before the convergence properties analysis, we have

Lemma 1. For a given antenna position vector $(\mathbf{L}_{Tk}, \mathbf{L}_{Rk})$, the power allocation problem can be rewritten as a convex optimization problem.

Proof. Same as Appendix A. \square

Lemma 2. Based on the given power allocation scheme \mathbf{P}_{Tk} , the antenna deployment solution of the local search is the optimal scheme [19].

The closed-loop scheme consists of the two local search algorithms described above and optimizes the $(\mathbf{L}_{Tk}, \mathbf{L}_{Rk})$ and \mathbf{P}_{Tk} in each loop, respectively. In each iteration, the local search algorithm for antenna placement is based on the optimal power solution from the last cycle. Instead, its current placement scheme serves as an input parameter for power allocation, obtaining the initial power value for the next cycle by convex optimization solving.

In summary, the optimization is accomplished by selecting the locations of transmitting and receiving antennas, and then completing the optimal transmit power allocation. On this basis, the joint optimization problem can be solved by using a two-staged algorithm and cyclic optimization, and the cycle terminates to the optimum once satisfying convergence conditions [29,30,39]. This scheme ultimately improves the overall network target detection performance, so that a closed loop is generated. The solution steps summary is given in Figure 3.

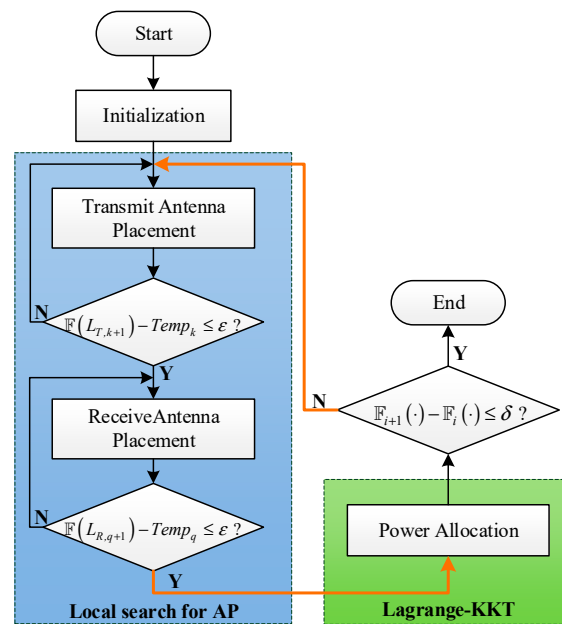


Figure 3. Block diagram of the closed-loop scheme.

3.4. Computational Complexity Analysis

The proposed JAPPA strategy mainly contains two phases that are as follows:

- (1) The local search for antenna placement;
- (2) The Lagrange-KKT for Power Allocation.

Strictly speaking, the computational complexity of the proposed optimization model solving algorithm is mainly determined by the number of iterations of the antenna position selection problem and in the proposed local search method, the exploration for a better antenna placement can be via swapping in and out more points. Therefore, the proposed antenna placement method is with a worst-case computational complexity of $\mathcal{O}((M + N)Q^3)$, wherein Q is the number of selectable coordinate points in the area. Additionally, when the antenna position vectors in (34) are determined, they become convex. At that time, with the Lagrangian-KKT method having a complexity of $\mathcal{O}(MN)$ in each optimization round [37], the JAPPA method computational complexity can be evaluated as $\mathcal{O}((M + N)Q^3 + MN)$. For comparison, the exhaustive search algorithm [23] is with the worst-case complexity of $\mathcal{O}((C_Q^{M+N} / (M!N!))MN) \approx \mathcal{O}(Q^{M+N}MN)$, which possesses a much heavier computational burden and the optimization method TWANPA, proposed in [19], has a polynomial computational burden of $\mathcal{O}(MQ^2(NQ + 1) + N^2)$. Therefore, we list the calculation complexity comparison given in Table 1.

Table 1. Computational complexity comparison.

| Algorithm | Exhaustive Search | TWANPA Method | JAPPA Strategy |
|--------------------------|--------------------------|-----------------------------------|--------------------------------|
| Computational complexity | $\mathcal{O}(Q^{M+N}MN)$ | $\mathcal{O}(MQ^2(NQ + 1) + N^2)$ | $\mathcal{O}((M + N)Q^3 + MN)$ |

4. Simulation Results and Discussion

In this section, the simulation results and numerical analysis are presented to demonstrate the effectiveness of the proposed JAPPA strategy. Herein, in our simulation, a 3×3 MIMO radar network ($M = 3$ transmitters and $N = 3$ receivers) is assumed to be placed in a square-shaped plane with sides equal to 20 km. We ignore the electromagnetic coupling between widely separated antennas, and we assume the Swerling I model for the target RCS fluctuation. In addition, to simulate the combat scenario of realistic air defense confrontation, we define a priority level ranging from approximately 0 to 1 for the whole square from the perspective of target detection. As Figure 4 shows, we randomly set an irregular priority level at each grid point, which will be utilized as the weighting coefficient to measure the target detection capability. In addition, the relevant radar parameters used in the simulation are given in Table 2.

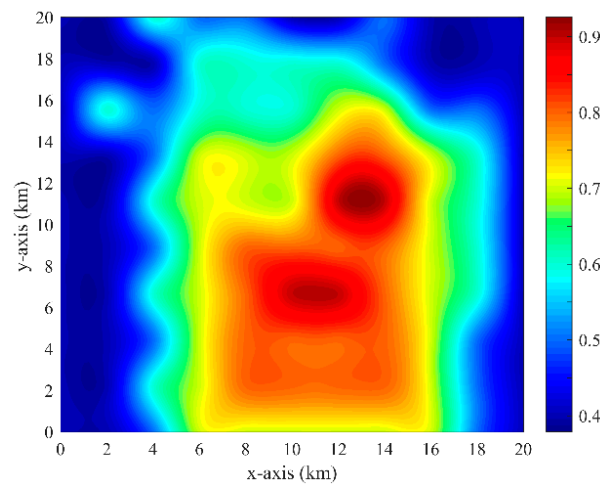


Figure 4. Priority level.

Table 2. System parameters.

| Names | Symbols | Settings |
|-------------------------------|--------------|------------------|
| Transmitting Antenna Gain | G_m | 30 dB |
| Receiving Antenna Gain | G_n | 30 dB |
| Processing Gain At Receiver | I_p | 20 dB |
| Carrier Frequency | f_c | 10 GHz |
| Target Average RCS | σ_0^2 | 2 m ² |
| Radar Network Scattering Loss | L_c | 0 dB |
| Radar Network Receiving Loss | L_r | 0 dB |
| Noise Factor | F_n | 4 dB |
| Bandwidth | B | 5 MHz |
| Transmit Power | P_{TOTAL} | 30 KW |
| Minimum Transmit Power | P_{Tmin} | 0 KW |
| Maximum Transmit Power | P_{Tmax} | 30 KW |

The echo SNR is an essential evaluation indicator of a radar system to evaluate its target detection performance. We calculate the average SNR of the radar system by calculating the SNR of each grid point and the echo SNR is given as

$$SNR = E\{\mathbf{y}_n | \mathcal{H}_1\} - E\{\mathbf{y}_n | \mathcal{H}_0\} \quad (46)$$

Moreover, the corresponding detection probability (P_D) of the radar network at the k -th iteration is defined as [40].

$$P_{D_k} \approx 0.5 \times \operatorname{erfc}\left(\sqrt{-\ln P_{fa}} - \sqrt{\operatorname{SNR}_k + 0.5}\right) P_{D_k} \approx 0.5 \times \operatorname{erfc}\left(\sqrt{-\ln P_{fa}} - \sqrt{\operatorname{SNR}_k + 0.5}\right) \quad (47)$$

where complementary error function erfc is formulated as

$$\operatorname{erfc}(z) = 1 - \frac{1}{\sqrt{\pi}} \int_0^z e^{-v^2} dv \quad (48)$$

Subsequently, to tackle the initialization of the optimization circulation, we firstly fix the transmitters' position parameters to optimize the remaining two parameters. Three transmitter antennas are placed at the lowest system radiation power density point one after another [19]. Therefore, the initial transmitting antenna positions are shown in Table 3 and our simulations are run in MATLAB 2019a on a computer with a 2.60 GHz CPU and 16.0 GB RAM. 16.0 GB.

Table 3. Initial transmitting antennas positions.

| Transmitter | x (km) | y (km) |
|-------------|--------|--------|
| #1 | 14 | 10 |
| #2 | 2 | 14 |
| #3 | 4 | 18 |

At this point, we utilize the initial transmitting antennas position scheme for the first iterative to start the iteration optimization loop. The positions are chosen one by one according to the weighted NP-based log-LRT and converge to the optimal strategy after six iterations of optimization. The result of receiver and transmitter coordinate positions is shown in Tables 4 and 5, respectively. Further, the optimal power allocation scheme and antenna geometry are shown in Table 6 and Figure 5, respectively.

Table 4. Transmitting antennas positions.

| Transmitter | x (km) | y (km) |
|-------------|--------|--------|
| #1 | 4 | 2 |
| #2 | 10 | 6 |
| #3 | 14 | 10 |

Table 5. Receiving antennas positions.

| Transmitter | x (km) | y (km) |
|-------------|--------|--------|
| #1 | 16 | 8 |
| #2 | 12 | 12 |
| #3 | 8 | 4 |

Table 6. Receiving antennas positions.

| Transmitter | #1 | #2 | #3 |
|-----------------------|-------|-------|--------|
| Power Allocation (KW) | 0.133 | 5.744 | 24.123 |

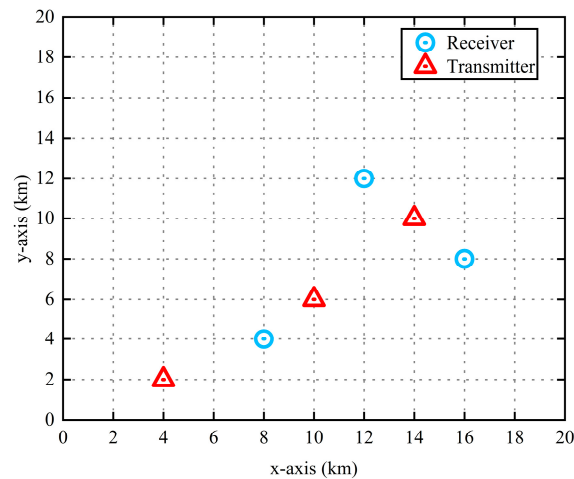


Figure 5. Optimal antennas' geometry distribution.

The resulting transmitting power allocated to the transmitters over 15 iterations is present in Figure 6. The power allocation values remain stable after the five iterations, which verified the algorithm's convergence inferred in the previous paper. The transmitting antenna #2 has the highest priority level of the plane, so it receives more power resources than the other two antennas. The relatively large distance between the transmitting antenna #1 and the rest of the radars and its inferior priority position results in a lower allocated power level.

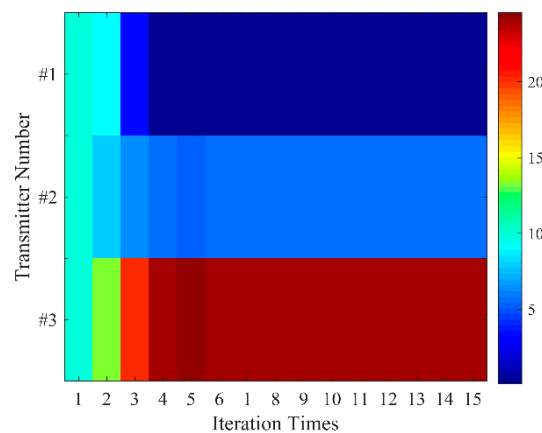


Figure 6. Power allocation results over 15 iterations.

4.1. Factors That Affect the Results of Iterative Optimization

4.1.1. Case 1: Optimization Parameters' Degree of Freedom

In principle, expanding the freedom of optimizing parameters can effectively improve the operational performance of radar systems. Here, we discuss the effect of optimization parameters' degree of freedom (DOF). There are three DOFs regarding antenna placement and power allocation: the positions of the transmitting antenna, the positions of the receiving antennas, and the transmitting power. In this case, separate optimization and combinatorial optimization of antenna placements and power allocation are carried out to analyze the different detection performance improvements, respectively. The following groups of different optimization objects will be investigated separately.

1. Single-parameter optimization:

- (1) *Transmitting antenna position optimization (TAO)*: The approach simply adjusts the location of the transmitting antenna to enhance the radar network's target detection capacity.

- (2) *Receiving antenna position optimization (RAO)*: The radar network transmitter sites remain constant with evenly distributed transmitting power, and only the placements of the receiving antennas are modified to improve the radar network's detecting capability.
 - (3) *Transmit power allocation optimization (TPO)*: The transmitting power is efficiently allocated to increase target detection capabilities based on the random deployment of the radar network antenna space architecture.
2. Two-element optimization:
- (1) *Joint antenna placement optimization (JAP)*: In this experiment, the transmitting power is uniformly distributed and the antenna deployment positions are optimized using a two-stage method, in which transmitting and receiving antenna positions are iteratively optimized. The iteration completes when the increment reaches the given error limit.
 - (2) *Joint transmitter placement and power allocation optimization (JTTPA)*: We jointly design the transmit power allocation and transmitters' placement to optimize radar performance criteria.

Figure 7 compares the radar target detection performance by the receiver-operating characteristic (ROC) curves of different optimization methods. The larger the area under the curve, the higher the SNR of the radar network, which implies better target detection performance. It can be observed that the optimal transmitting power allocation with random antenna placement disregards the importance of location and the priority level and, thus, TPO provides the worst detection performance. By contrast, the optimization considering the antenna placement with the same power has a slightly better effect. The JAP and JTTPA ROC curves indicate that addressing the power allocation and antenna deployment simultaneously can significantly improve the performance of the radar network. The suboptimal two-element optimization method has an overall higher ability to improve radar performance than the single-parameter optimization method. Furthermore, it can be seen that the proposed JAPPA method optimizes three parameters simultaneously to improve detection ability, thus, providing the most superior detection performance.

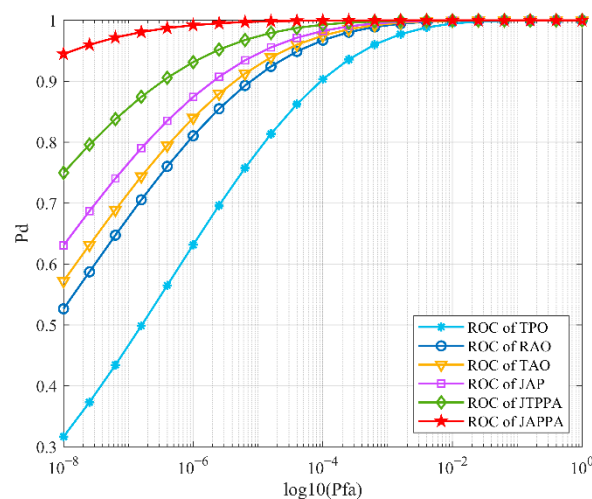


Figure 7. Average ROC curves for power allocation method.

4.1.2. Case 2: Iterative Loop Containment Range

This case investigates the effect of iterative loop range on resource allocation, and further analyzes the joint optimization problem of antenna placement and power allocation in distributed MIMO radar networks, focusing on the collaborative optimization of optimizing power allocation and antenna location problem.

Two experiments are carried out: Iterative optimization of antenna placement (IOAP), an algorithm that first iteratively optimizes the antenna position and finally optimizes the power allocation, and iterative loop of antenna position and power distribution (JAPPA). The optimization difference between the two iterative loops is shown in Figure 8a. The first separation of the two dotted lines is due to the JAPPA method performing the optimal power allocation, while IOAP executes the next round of antenna position optimization deployment. Finally, both the curves terminate the optimization process after satisfying the convergence conditions. Figure 8b gives an SNR comparison of the two algorithms, demonstrating that JAPPA can more fully use the limited resources to enhance the system.

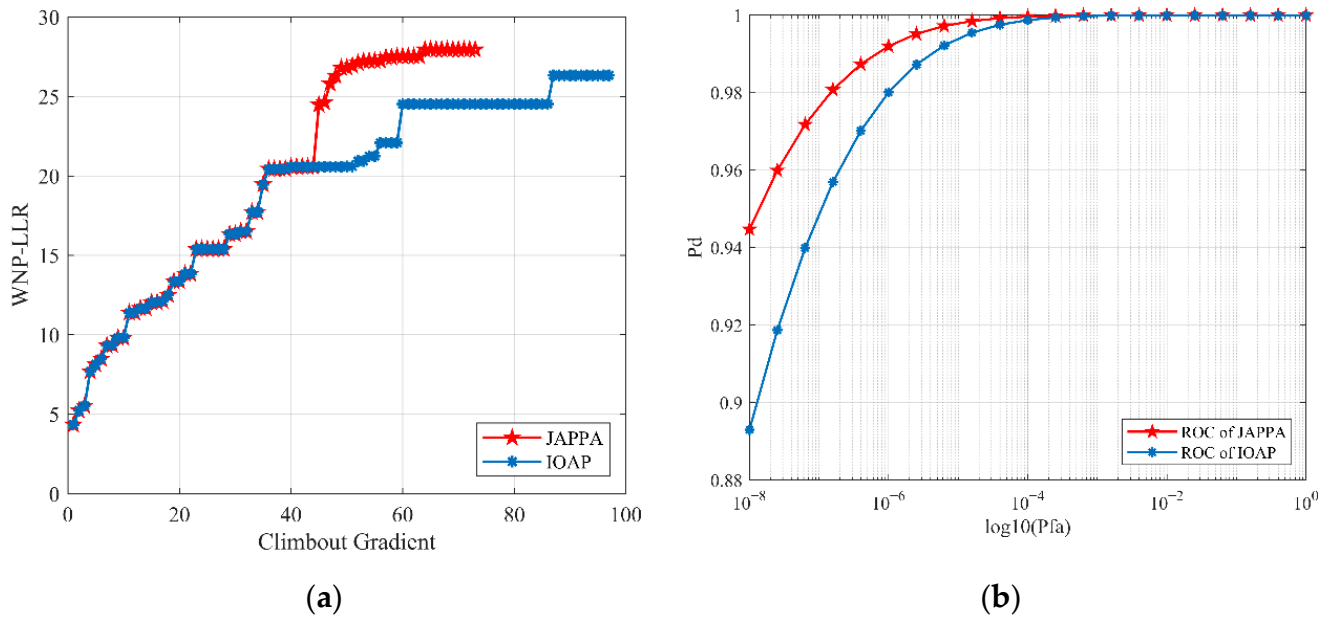


Figure 8. Simulation results comparison (a) optimum iterative process; (b) average ROC curves for IOAP and JAPPA.

The IOAP antenna placement scheme is given in Tables 7 and 8. Figure 9a illustrates the resulting antenna geometry distribution in the square-shaped plane and Figure 9b presents the solution for the power allocation problem and compares the power allocation schemes of the IOPA and JAAPA methods. The transmitting antenna with the highest power allocation is located at the same location compared to the JAPPA scheme. The essence is that the point has the highest priority, and its results also justify the optimization results.

Table 7. Transmitting antennas positions.

| Transmitter | x (km) | y (km) |
|-------------|--------|--------|
| #1 | 18 | 14 |
| #2 | 10 | 6 |
| #3 | 14 | 10 |

Table 8. Receiving antennas positions.

| Transmitter | x (km) | y (km) |
|-------------|--------|--------|
| #1 | 16 | 12 |
| #2 | 12 | 8 |
| #3 | 8 | 4 |

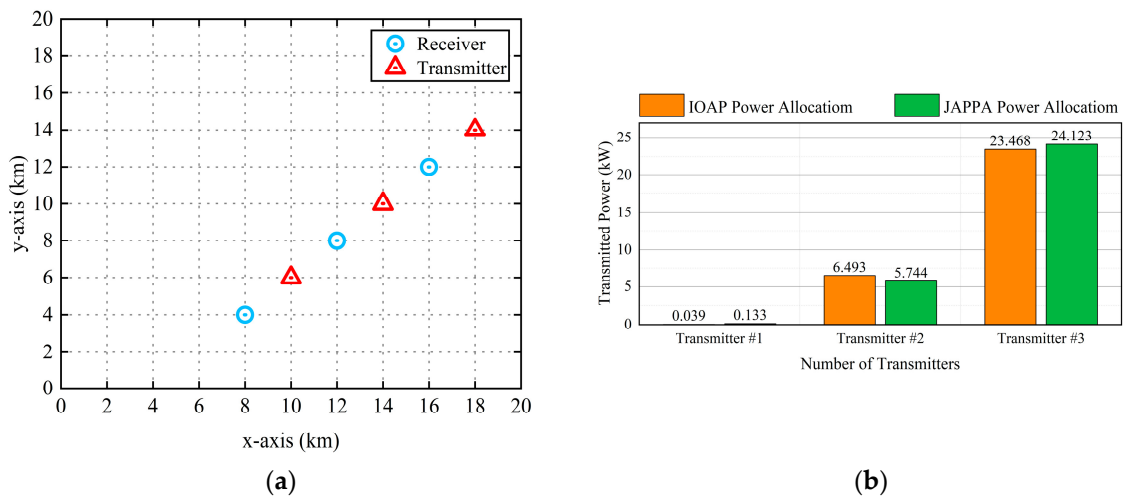


Figure 9. Optimal scheme based on IOAP. (a) IOAP Antennas' geometry distribution; (b) IOAP power assigned to the transmitters.

4.1.3. Case 3: Numbers of Antennas

Obviously, improvements such as raising the transmitting power, improving the antenna gain, and increasing the amount of system equipment can enhance detection performance [9,25]. This simulation is extended to the different numbers of the transmitting and receiving antennas, and the effect of different antenna quantities to complete the target detection task under the constraint of power resource budget has been investigated.

The curves in Figure 10 represent different numbers of transceiver stations, and the detection probability varies with the probability of false alarms. The results indicate that with the increase in the antenna amounts, the radar network possesses a superior detection performance due to the SNR improvement brought by the diversity gain. However, the target detection performance of radar networks under power constraints is not always positively correlated with the number of antennas. Since the radar network detection performance of $M = 3, N = 2$ is superior to that of $M = 3, N = 3$, the optimal antennas quantity scheme for monitoring in a particular area is not superior in number. It deserves further research since it has significant guiding relevance for practical applications.

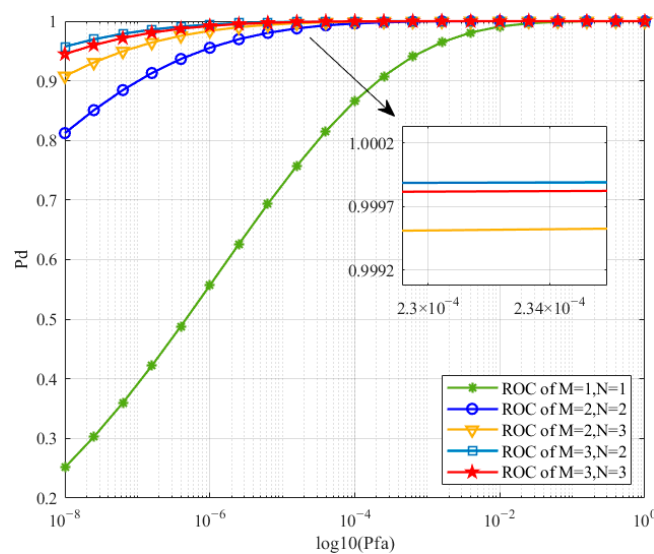


Figure 10. Average ROC curves for different antenna amounts.

4.2. The Efficiency of the Iterative Two-Stage Closed-Loop Solver

In this section, the time efficiency of the proposed method is illustrated using the exhaustive search-based algorithm as a benchmark. In Figure 11a, it can be observed that the SNR performance of JAPPA is close to that of the exhaustive method, which proves the effectiveness of JAPPA. The threshold $\varepsilon = 10^{-6}$ is set for each iteration increment to fairly compare the computational complexity. Then, the running time of the algorithm is calculated by Monte Carlo experiments, and a visual comparison is shown in Figure 11b. Specifically, it separately takes the exhaustive search method and the TWANPA method about 10^5 and 3×10^2 s to complete optimization. By contrast, the proposed two-staged JAPPA algorithm only takes about 2×10^2 s in problem solving. That implies the proposed JAPPA method can provide comparable performance to the exhaustive search method while less time-consuming than the TWANPA and conforms to the complex conclusion in Table 1.

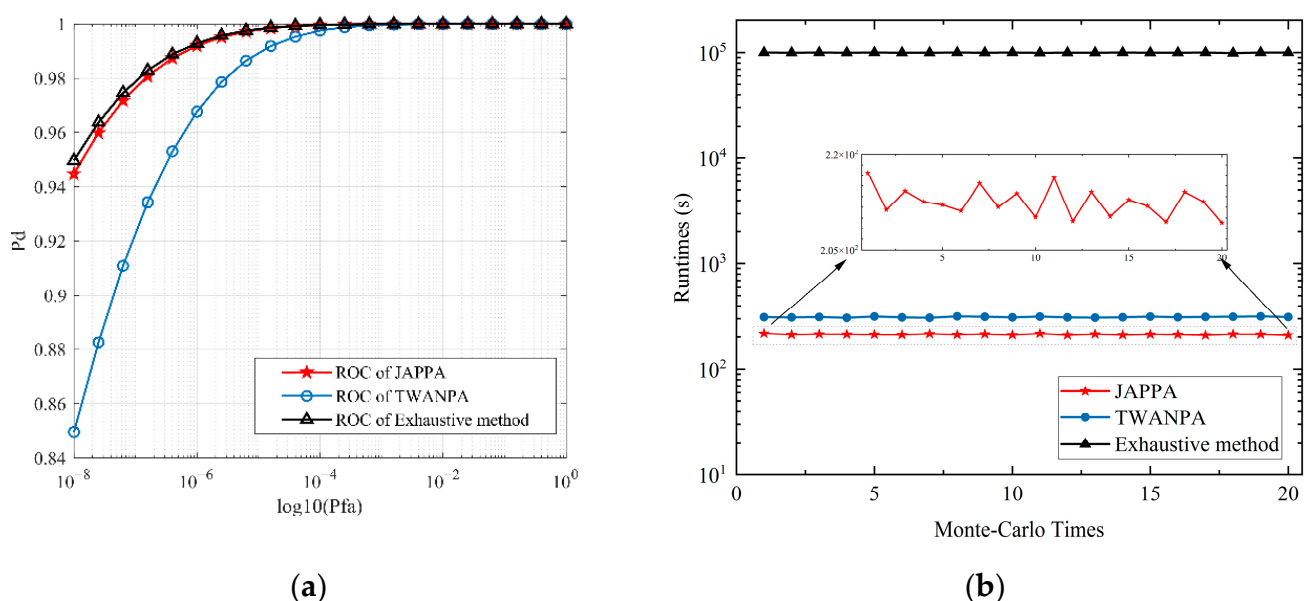


Figure 11. Performance comparison of TWANPA, the exhaustive search, and the JAPPA: (a) average ROC curves; (b) runtime.

4.3. Effectiveness of the Proposed Method

In this part, the effectiveness of the proposed JAPPA technique is analyzed with three comparative tests by evaluating the degree of optimization of the algorithm on the radar target recognition performance.

1. *Random antenna placement with uniform power allocation* (RAP-UPA): This method randomly selects the positions of the antennas with the uniform transmitting power resource allocation.
2. *Random antenna placement with non-uniform power allocation* (RAP-UUPA): The realistic scenario of non-uniform power allocation and random antenna placement will be considered in this simulation.
3. *Optimal antenna placement with uniform power allocation* (OAP-UPA) [13]: In this scenario, the transmitters and receivers are optimally placed sequentially with the power consumption uniformly allocated to the transmitting antennas.
4. *Three-stage water-filling-type antenna placement and power allocation strategy* (TWANPA) [19]: This method improves the radar detection performance through successive optimization under the total power constraint and designs a suboptimal method to effectively locate transmitting and receiving antennas under the water-filling power allocation. It completes the transmitting antenna placement using the power density criterion and positioning the receiving antenna with the SNR criterion. Subsequently, a closed-loop

optimization mechanism is established by repeating the antennas' positions using the allocated powers.

The simulation results in Figure 12 present the ROC comparison between the proposed JAPPA strategy and the other four benchmarks. Therefore, it is apparent from a brief look at Figure 12 that the superior performance of the proposed JAPPA strategy is very significant to improve the SNR of the radar system. Among these four benchmarks, OAP-UPA outperforms RAP-UPA and RAP-UUPA due to the optimal antenna positions at both the transmitter and receiver end. TWANPA shows advantages over the OAP-UPA and achieves superior detection performance, since it uses an optimal power allocation scheme based on the water-filling-type method. The TWANPA method selects the optimal antenna placement set based on two different objective functions and iteratively converges to a suboptimal solution, while the proposed JAPPA method completes the optimization based on a unified log-LRT function. The result verifies the effectiveness of the established optimization model.

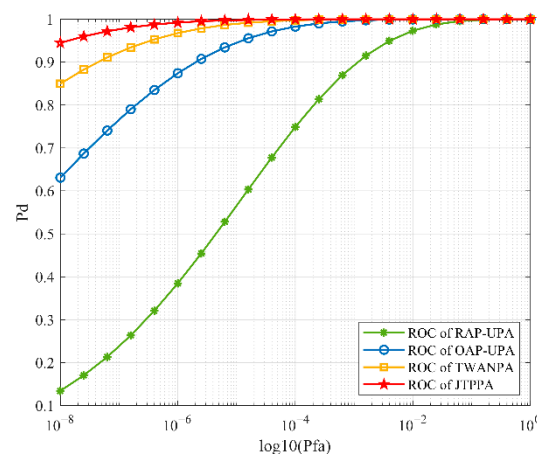


Figure 12. Average ROC curves for five power allocation methods.

5. Conclusions

In this paper, the joint resource allocation problem of a distributed MIMO radar network based on environmental information is investigated and an optimization scheme JAPPA is developed to maximize the detection performance of the radar system for the whole surveillance area. The intractable mixed-integer programming problem is modified into a two-stage optimization problem, which is solved by the greedy take-away method and the Lagrangian-KKT method, respectively. Finally, the jointly optimal solution is guaranteed using a closed-loop scheme and the simulation results demonstrate the superiority of the proposed JAPPA method and show the following aspects.

1. The log-LRT function unifies the antenna position variables and transmitter power allocation variables into a single collaborative objective function, which is suitable for guiding the joint resource allocation optimization.
2. The joint antenna and power allocation optimization can more effectively improve the target detection performance of the radar system.
3. The proposed strategy is effective and efficient in solving the JAPPA problem.

Future research could consider more environmental factors, such as terrain, clutter distribution, etc., to get closer to the actual battlefield environment [41,42], and extend to dynamic target detection and joint detection and tracking [43,44]. Beyond that, game theory [45] and machine learning may be taken into account.

Author Contributions: Conceptualization, C.Q.; methodology, C.Q.; validation, C.Q.; formal analysis, C.Q.; investigation, C.Q.; resources, C.Q. and J.X.; data curation, C.Q.; writing—original draft prepa-

ration, C.Q.; writing—review and editing, J.X. and H.Z.; visualization, C.Q. and H.Z.; supervision, J.X. and H.Z. All authors have read and agreed to the published version of the manuscript.

Funding: This research was funded by the National Natural Science Foundation of China, grant number 62001506.

Data Availability Statement: Not applicable.

Acknowledgments: The authors would like to thank the Associate Editor and all the reviewers for their valuable and insightful comments and suggestions during the revision of this work.

Conflicts of Interest: The authors declare no conflict of interest.

Appendix A

Prove that Formula (42) is a convex optimization model.

The constraint in the Formula (42) is linear and convex. The objective function is rewritten as follows:

$$\mathbb{F}(\mathbf{P}_T) = \sum_{m=1}^M \sum_{n=1}^N \left[\text{Ln} \left(\sqrt{2\pi} \cdot \frac{E_{nm} c_{nm}}{\sigma} \cdot \exp \left(\frac{E_{nm} c_{nm}^2}{2\sigma^2} \right) \right) - \text{Ln} \left(1 + \frac{E_{nm} c_{nm}^2}{\sigma^2} \right) \right] \quad (\text{A1})$$

To simplify the calculation process, we have

$$\mathbb{G} = \text{Ln} \left(\sqrt{2\pi} \cdot \frac{c_{nm} \sqrt{L_{nm} P_{Tm}}}{\sigma} \cdot \exp \left(\frac{c_{nm}^2 L_{nm} P_{Tm}}{2\sigma^2} \right) \right) - \text{Ln} \left(1 + \frac{c_{nm}^2 L_{nm} P_{Tm}}{\sigma^2} \right) \quad (\text{A2})$$

It is necessary to derive the second derivative of \mathbb{G}

$$\nabla_{P_m}^{P_m} \mathbb{G} = \frac{2P_{Tm}^2 \cdot \left(\frac{c_{nm}^2 L_{nm}}{\sigma^2} \right)^2 - \left(1 + \frac{c_{nm}^2 L_{nm}}{\sigma^2} \cdot P_{Tm} \right)^2}{2P_{Tm}^2 \cdot \left(1 + \frac{c_{nm}^2 L_{nm}}{\sigma^2} \cdot P_{Tm} \right)^2} \quad (\text{A3})$$

where $\nabla_{P_m}^{P_m}$ denotes the second partial derivative with regard to P_m . From the literature [36], if the second derivative of a one-variable function is always non-negative in the feasible region, the function is convex. At this point, only the sign of the numerator needs to be considered and it is easy to prove that in the case of the actual radar power consumption order of magnitude, $\nabla_{P_m}^{P_m} \mathbb{G}$ is always positive and $\mathbb{F}(\mathbf{P}_T)$ can be regarded as the affine transformation of \mathbb{G} with respect to P_m . Therefore, $\mathbb{F}(\mathbf{P}_T)$ is convex. That is, problem (45) is a convex optimization problem [23].

The certificate is completed.

References

1. Fishler, E.; Haimovich, A.; Blum, R.; Chizhik, D.; Cimini, L.; Valenzuela, R. MIMO radar: An idea whose time has come. In Proceedings of the 2004 IEEE Radar Conference (IEEE Cat. No.04CH37509), Philadelphia, PA, USA, 29 April 2004; pp. 71–78.
2. Yang, J.; Aubry, A.; Maio, A.D.; Yu, X.; Cui, G. Design of Constant Modulus Discrete Phase Radar Waveforms Subject to Multi-Spectral Constraints. *IEEE Signal Process. Lett.* **2020**, *27*, 875–879. [\[CrossRef\]](#)
3. Yao, Y.; Liu, H.T.; Miao, P.; Wu, L.N. MIMO Radar Design for Extended Target Detection in a Spectrally Crowded Environment. *IEEE Trans. Intell. Transp. Syst.* **2021**, 1–10. [\[CrossRef\]](#)
4. Stoica, P. *MIMO Radar Signal Processing*; Wiley-IEEE Press: Hoboken, NJ, USA, 2009.
5. Li, X.; Chen, H.; Zhuang, Z.; Yang, J.; Qiu, Z. Effects of transmitting correlated waveforms for co-located multi-input multi-output radar with target detection and localisation. *Signal Process. IET* **2013**, *7*, 897–910.
6. Haimovich, A.M.; Blum, R.S.; Cimini, L.J. MIMO Radar with Widely Separated Antennas. *IEEE Signal Process. Mag.* **2008**, *25*, 116–129. [\[CrossRef\]](#)
7. Gogineni, S.; Nehorai, A. Target Estimation Using Sparse Modeling for Distributed MIMO Radar. *IEEE Trans. Signal Process.* **2011**, *59*, 5315–5325. [\[CrossRef\]](#)
8. Fishler, E.; Haimovich, A.; Blum, R.S.; Cimini, L.J.; Chizhik, D.; Valenzuela, R.A. Spatial Diversity in Radars—Models and Detection Performance. *IEEE Trans. Signal Process.* **2006**, *54*, 823–838. [\[CrossRef\]](#)

9. He, Q.; Blum, R.S.; Haimovich, A.M. Noncoherent MIMO Radar for Location and Velocity Estimation: More Antennas Means Better Performance. *IEEE Trans. Signal Process.* **2010**, *58*, 3661–3680. [[CrossRef](#)]
10. Godrich, H.; Haimovich, A.M.; Blum, R.S. Cramer Rao bound on target localization estimation in MIMO radar systems. In Proceedings of the 2008 42nd Annual Conference on Information Sciences and Systems, Princeton, NJ, USA, 19–21 March 2008; pp. 134–139.
11. Gacho, J.F.A.L. Researching UAV Threat—New Challenges. In Proceedings of the 2021 International Conference on Military Technologies (ICMT), Brno, Czech Republic, 8–11 June 2021; pp. 1–6.
12. Yao, Y.; Wu, L.; Liu, H.T. Robust Transceiver Design in the Presence of Eclipsing Loss for Spectrally Dense Environments. *IEEE Syst. J.* **2021**, *15*, 4334–4345. [[CrossRef](#)]
13. Yi, J.; Wan, X.; Leung, H.; Lü, M. Joint Placement of Transmitters and Receivers for Distributed MIMO Radars. *IEEE Trans. Aerosp. Electron. Syst.* **2017**, *53*, 122–134. [[CrossRef](#)]
14. Chitgarha, M.M.; Radmard, M.; Majd, M.N.; Nayebi, M.M. Improving MIMO radar’s performance through receivers’ positioning. *IET Signal Process.* **2017**, *11*, 622–630. [[CrossRef](#)]
15. Wang, Y.; Yang, S.; Zhou, T.; Li, N. Geometric Optimization of Distributed MIMO Radar Systems with Spatial Distance Constraints. *IEEE Access* **2020**, *8*, 199227–199241. [[CrossRef](#)]
16. Feng, H.Z.; Liu, H.W.; Yan, J.K.; Dai, F.Z.; Fang, M. A fast efficient power allocation algorithm for target localization in cognitive distributed multiple radar systems. *Signal Process.* **2016**, *127*, 100–116. [[CrossRef](#)]
17. Yan, J.; Pu, W.; Liu, H.; Jiu, B.; Bao, Z. Robust Chance Constrained Power Allocation Scheme for Multiple Target Localization in Colocated MIMO Radar System. *IEEE Trans. Signal Process.* **2018**, *66*, 3946–3957. [[CrossRef](#)]
18. Shi, C.G.; Wang, Y.J.; Wang, F.; Salous, S.; Zhou, J.J. Power resource allocation scheme for distributed MIMO dual-function radar-communication system based on low probability of intercept. *Digit. Signal Prog.* **2020**, *106*, 12. [[CrossRef](#)]
19. Radmard, M.; Chitgarha, M.M.; Majd, M.N.; Nayebi, M.M. Antenna placement and power allocation optimization in MIMO detection. *IEEE Trans. Aerosp. Electron. Syst.* **2014**, *50*, 1468–1478. [[CrossRef](#)]
20. Jebali, S.; Keshavarz, H.; Allahdadi, M. Joint Power allocation and target detection in distributed MIMO radars. *IET Radar Sonar Navig.* **2021**, *15*, 1433–1447. [[CrossRef](#)]
21. Ma, B.; Chen, H.; Sun, B.; Xiao, H. A Joint Scheme of Antenna Selection and Power Allocation for Localization in MIMO Radar Sensor Networks. *IEEE Commun. Lett.* **2014**, *18*, 2225–2228. [[CrossRef](#)]
22. Xie, M.C.; Yi, W.; Kirubarajan, T.; Kong, L.J. Joint Node Selection and Power Allocation Strategy for Multitarget Tracking in Decentralized Radar Networks. *IEEE Trans. Signal Process.* **2018**, *66*, 729–743. [[CrossRef](#)]
23. Godrich, H.; Petropulu, A.P.; Poor, H.V. Sensor Selection in Distributed Multiple-Radar Architectures for Localization: A Knapsack Problem Formulation. *IEEE Trans. Signal Process.* **2012**, *60*, 247–260. [[CrossRef](#)]
24. Berenguer, I.; Xiaodong, W.; Krishnamurthy, V. Adaptive MIMO antenna selection via discrete stochastic optimization. *IEEE Trans. Signal Process.* **2005**, *53*, 4315–4329. [[CrossRef](#)]
25. He, Q.; Blum, R.S.; Haimovich, A.M.; He, Z. Antenna placement for velocity estimation using MIMO radar. In Proceedings of the 2008 42nd Asilomar Conference on Signals, Systems and Computers, Pacific Grove, CA, USA, 26–29 October 2008; pp. 619–623.
26. Ajorloo, A.; Amini, A.; Tohidi, E.; Bastani, M.H.; Leus, G. Antenna Placement in a Compressive Sensing-Based Colocated MIMO Radar. *IEEE Trans. Aerosp. Electron. Syst.* **2020**, *56*, 4606–4614. [[CrossRef](#)]
27. Yuan, Y.; Yi, W.; Hoseinnezhad, R.; Varshney, P.K. Robust Power Allocation for Resource-Aware Multi-Target Tracking with Colocated MIMO Radars. *IEEE Trans. Signal Process.* **2021**, *69*, 443–458. [[CrossRef](#)]
28. Chavali, P.; Nehorai, A. Scheduling and Power Allocation in a Cognitive Radar Network for Multiple-Target Tracking. *IEEE Trans. Signal Process.* **2012**, *60*, 715–729. [[CrossRef](#)]
29. Zhang, H.W.; Liu, W.J.; Xie, J.W.; Zhang, Z.J.; Lu, W.L. Joint Subarray Selection and Power Allocation for Cognitive Target Tracking in Large-Scale MIMO Radar Networks. *IEEE Syst. J.* **2020**, *14*, 2569–2580. [[CrossRef](#)]
30. Shia, C.; Ding, L.; Wang, F.; Zhou, J.; Yan, J. Collaborative radar node selection and transmitter resource allocation algorithm for target tracking applications in multiple radar architectures. *Digit. Signal Prog.* **2022**, *121*, 103318. [[CrossRef](#)]
31. Zhang, H.; Xie, J.; Shi, J.; Zhang, Z.; Fu, X. Sensor Scheduling and Resource Allocation in Distributed MIMO Radar for Joint Target Tracking and Detection. *IEEE Access* **2019**, *7*, 62387–62400. [[CrossRef](#)]
32. Skolnik, M.I. *Radar Handbook*; McGraw-Hill Education: New York, NY, USA, 1990.
33. News, S.; News, S. *Detection, Estimation and Modulation Theory*; John Wiley & Sons, Inc.: Hoboken, NJ, USA, 1968.
34. Yuan, Y.; Yi, W.; Kirubarajan, T.; Kong, L.J. Scaled accuracy based power allocation for multi-target tracking with colocated MIMO radars. *Signal Process.* **2019**, *158*, 227–240. [[CrossRef](#)]
35. Yan, J.K.; Liu, H.W.; Jiu, B.; Chen, B.; Liu, Z.; Bao, Z. Simultaneous Multibeam Resource Allocation Scheme for Multiple Target Tracking. *IEEE Trans. Signal Process.* **2015**, *63*, 3110–3122. [[CrossRef](#)]
36. Boyd, S.; Vandenberghe, L. *Convex Optimization*; Cambridge University Press: Cambridge, UK, 2004.
37. Boyd, S.; Vandenberghe, L.; Faybusovich, L. Convex Optimization. *IEEE Trans. Autom. Control.* **2006**, *51*, 1859.
38. Bertsekas, D.P.; Nedic, A.; Ozdaglar, A.E. *Convex Analysis and Optimization*; Pitman Advanced Pub. Program; MIT: Cambridge, MA, USA, 2003.
39. Stoica, P.; Selen, Y. Cyclic minimizers, majorization techniques, and the expectation-maximization algorithm: A refresher. *IEEE Signal Process. Mag.* **2004**, *21*, 112–114. [[CrossRef](#)]

40. Mahafza, B.R.; Elsherbeni, A. *MATLAB Simulations for Radar Systems Design*; Chapman and Hall/CRC: London, UK, 2003.
41. Liang, J.; Zhang, T.; Yang, Y.; Cui, G.; Yang, J. An efficient antenna placement method for MIMO radar under the situation of multiple interference regions. In Proceedings of the 2017 20th International Conference on Information Fusion (Fusion), Xi'an, China, 10–13 July 2017.
42. Zhang, H.; Liu, W.; Zhang, Z.; Lu, W.; Xie, J. Joint Target Assignment and Power Allocation in Multiple Distributed MIMO Radar Networks. *IEEE Syst. J.* **2020**, *15*, 694–704. [[CrossRef](#)]
43. Ristic, B.; Rosenberg, L.; Du, Y.K.; Wang, X.; Williams, J. A Bernoulli track-before-detect filter for maritime radar. *IET Radar Sonar Navig.* **2019**, *14*, 356–363. [[CrossRef](#)]
44. Zhang, H.; Liu, W.; Shi, J.; Fei, T.; Zong, B. Joint detection threshold optimization and illumination time allocation strategy for cognitive tracking in a networked radar system. *IEEE Trans. Signal Process.* **2022**. *to be published*.
45. He, B.; Su, H.; Huang, J. Joint Beamforming and Power Allocation Between A Multistatic MIMO Radar Network and Multiple Targets Using Game Theoretic Analysis. *Digit. Signal Prog.* **2021**, *115*, 103085. [[CrossRef](#)]